Development of Planning Framework for the Geometry Design of Continuous Flow Intersections

By

Xianfeng Yang (Corresponding Author)
Ph.D Candidate
Department of Civil & Environmental Engineering
University of Maryland
1173 Glenn L. Martin Hall,College Park, MD 20742
Tel: (301)-405-2638
Email: xyang125@umd.edu

Gang-Len Chang
Ph.D., Professor
Department of Civil & Environmental Engineering
University of Maryland
1173 Glenn L. Martin Hall,College Park, MD 20742
Tel: (301)-405-2638
Email: gang@umd.edu

Yang Lu
Ph.D Candidate
Department of Civil & Environmental Engineering
University of Maryland
1173 Glenn L. Martin Hall,College Park, MD 20742
Tel: (301)-405-7768
Email: yanglu83@umd.edu

Saed Rahwanji
Assistant Division Chief
Traffic Development & Support Division
Office of Traffic and Safety
Maryland State Highway Administration
Tel: (410)-787-5870
Email: srahwanji@sha.state.md.us

Word Count: 4326 + (6 figures + 6 table)*250 = 7,326 words

Submitted to the 2013 Transportation Research Board 92nd Annual Meeting and for publication on Transportation Research Record

ABSTRACT

Despite the increasing use of continuous flow intersections (CFI) to contend with the congestion caused by heavy through and left-turn traffic flows, a reliable and convenient tool for the traffic community to identify potential deficiencies for CFI's geometry design are not available yet. This is due to the unique geometric feature of CFI which comprises one primary intersection and several crossover intersections. The interdependent relation between the traffic delays and queues at a CFI's five closely-spaced intersections cannot be fully captured with the existing analysis models developed for conventional intersections. In response to such a need, this study presents a comprehensive analysis for the overall CFI delay, identifies the potential queue spillback locations, and develops a planning framework for CFI's geometry designs. To facilitate the application of our proposed models, this paper also includes a case study of a CFI at intersection MD 4 and MD 235 conducted by Maryland State Highway Administration.

INTRODUCTION

Continuous flow intersection (Referred as CFI) has attracted increasing attention during recent years. The main feature of CFI is to eliminate the conflict between left-turn and opposing through traffic by relocating the left-turn bay to several hundred feet upstream of the primary intersection so that the through and left-turn flows can move concurrently. With the presence of left-turn crossovers, a full CFI design with its primary and crossover intersections generally leads to a larger footprint than a typical conventional intersection. For a full CFI design, the primary intersection is located at the center, where four crossover intersections, also known as "left crossovers", are placed respectively on four approaching legs. Such a design allows all intersections in the CFI to operate with a two-phase signal control.

Due to the increasing applications of CFI over the past years, some fundamental issues associated with its operational efficiency and potential capacity have emerged as the priority research subjects. Goldblatt et al. *(1)* showed that the benefits of CFIs are particularly pronounced when the volumes to some approaches exceed the capacity of a conventional intersection. Using simulation data from CORSIM, Reid and Hummer *(2~5)* compared the performance of seven different unconventional designs with a conventional intersection under heavy left-turn volumes, and indicated that CFI has great potential to accommodate the heavy demand that has a high percentage of left-turn volume. Jagannathan *(6)* carried out a series of studies on the delay incurred at CFI, based on both the simulation and regression results.

In a later study, Seonyeong et al. *(7)* compared the performances of CFIs under balanced and unbalanced volume conditions, and reported that switching a conventional intersection to CFI can reduce the total delay approximately by 60% ~ 85% percent. Kim et al. *(8)* address initiative works done in the state of Maryland in order to provide a clearing house for unconventional arterial intersection designs (UAIDs) and apply their concepts to selected locations. Mohamed and Sayed (9) reported similar results and further argued that the capacity improvement of the CFI design is insensitive to an increase in the left-turn volume ratio. A field study by Pitaksringkarn *(10)* also confirmed that the CFI design can reduce the intersection delays and queues by 64 and 61 percents, respectively, during peak hours. The AIIR, published by the FHWA (11), reviews the geometric features, safety performance, operational efficiency, and construction cost of CFI.

In summary, existing studies *(12-14)* have generally concluded that CFI outperforms conventional intersection, especially under the high traffic demand and high left-turn volume scenarios. Nevertheless, many critical issues associated with CFI remain to be discussed. For instance, although many studies reported significant reduction in delay, the critical contributing factors as well as their respectively impacts on such performance improvement is not yet well identified. The correlation between intersection delay and key geometric features, such as bay length, was not studied. In fact, a CFI can be viewed as a small network comprising five intersection nodes and several interconnected links. Hence, the delays to different traffic movements are affected not only by the volume-to-capacity ratio at each intersection, but also by the queue lengths along all associated links. Although Mohamed and Sayed *(11)* pointed out that the improved capacity by CFI may be related to its unique geometric layout, no subsequent research is available along this direction.

The rest of this paper is organized as follows: Section 2 introduces the dataset for simulation experiments and performs the delay analysis for the full CFI design. A set of regression models for the queue length estimation are presented in Section 3. The details of the proposed planning framework are discussed in Section 4 respectively. A real-world case is studied in Section 5. Conclusions and on-going researches are summarized in Sections 6.

PERFORMANCE ANALYSIS

Despite existing studies have generally concluded that CFI outperforms conventional intersection, no in-depth analysis is completed for the performance evaluation of CFI. In this study, a comprehensive analysis of CFI delay is performed and some potential factors which may contribute to the intersection delay will be identified, based on the experimental data generated from VISSIM.

Experimental Design

Recognizing that a simulation system needs to faithfully reflect the behavior of its target driving populations, this study has conducted a field study at a CFI intersection (MD 210 & MD 228) to calibrate all key parameters embedded in VISSIM. The calibration of simulation parameters is performed by minimizing the following objective function:

$$\min \frac{1}{N}\sum_{i=1}^{N}(Q_{bi}-Q_{si})^2 \tag{1}$$

where, Q_{bi} is the observed maximum queue length at cycle i; Q_{si} denotes the simulated maximum queue length at cycle i; and N is the number of cycles observed;

The simulator calibration was conducted with a standard GA algorithm. TABLE 1 summarized the primary driving behavior parameters of VISSIM after calibrating with the field data.

TABLE 1 Driving Behavior Parameters of VISSIM

Parameters	**Value**
maximum acceleration	9.8 ft/s^2
desired acceleration	6.2 ft/s^2
look ahead distance	0 ~ 820 ft
probability of temporary lack of attention	10%
duration of temporary lack of attention	0.3s
average stand still distance	7.6 ft

To generate the experimental data with VISSIM, four scenarios with different geometric parameters are used to investigate its impact on the CFI's performance. TABLE 2 summarized the geometric parameters adopted in the simulation experiments.

TABLE 2 Geometric Parameters Used in Simulation Experiments

Geometric parameters / Case	**A**	**B**	**C**	**D**
Left-turn crossover spacing (feet)	200	300	400	500
Left-turn bay (feet)	250	350	450	550
Right-turn bay (feet)	300	300	300	300

Incoming traffic demands are generated from the most upstream end of those four CFI legs, where the simulation employs the Poisson process for traffic arrivals. A total of 600 volume sets are randomly generated for each scenario and simulated with VISSIM. To reduce the output variation due to the stochastic properties of microscopic simulation, each demand scenario has been simulated for 30 replications under different initial random seeds. The period of simulation for each case is set to 2 hours.

Delay Analysis of CFI

Jagannathan *(6)* derived the following delay model for CFI, assuming an exponential relation between average delay and traffic volumes:

$$d=\exp[a_0+(\sum_{ij} a_{ij}X_{ij})/10^4] \tag{2}$$

where X_{ij} represents the flow rates from approach i and movement group j. However, our experimental data reveals that the average delay depends not only on traffic volumes but also on the ratio between the maximum queue length and its corresponding link length at the intersection, as shown in FIGRUE 1 (A)~(C).

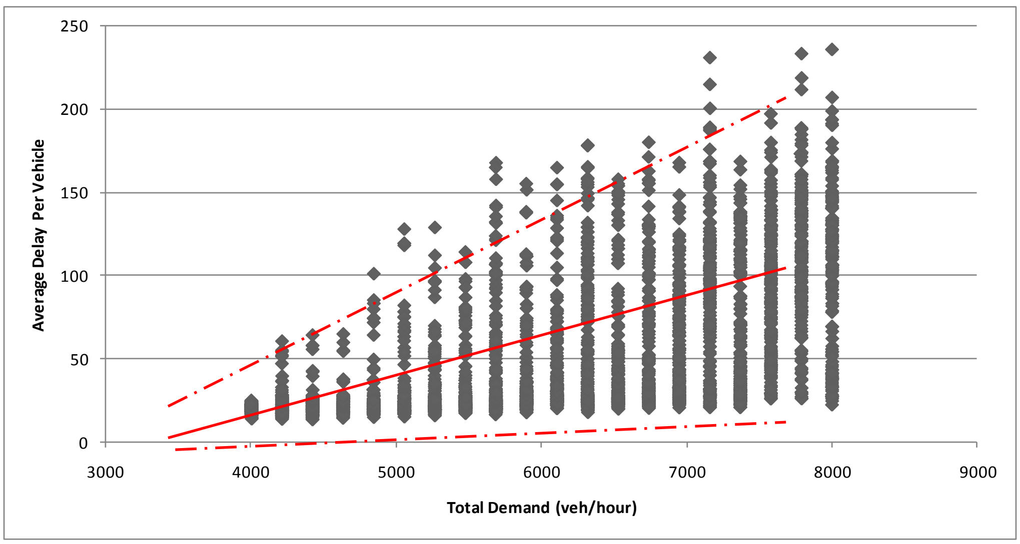

FIGURE 1(A) Scatter plot of average delay v.s. total demand

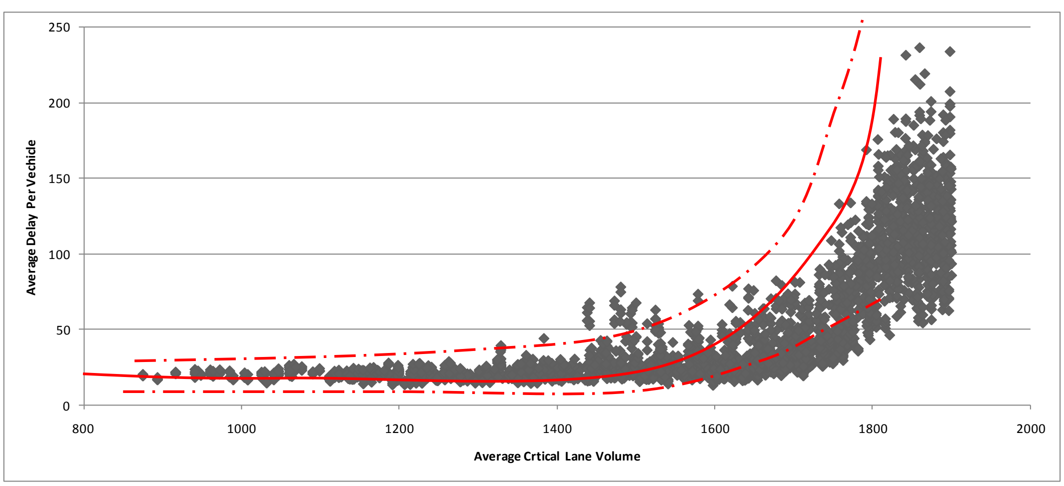

FIGURE 1(B) Scatter plot of average v.s. average critical lane volume

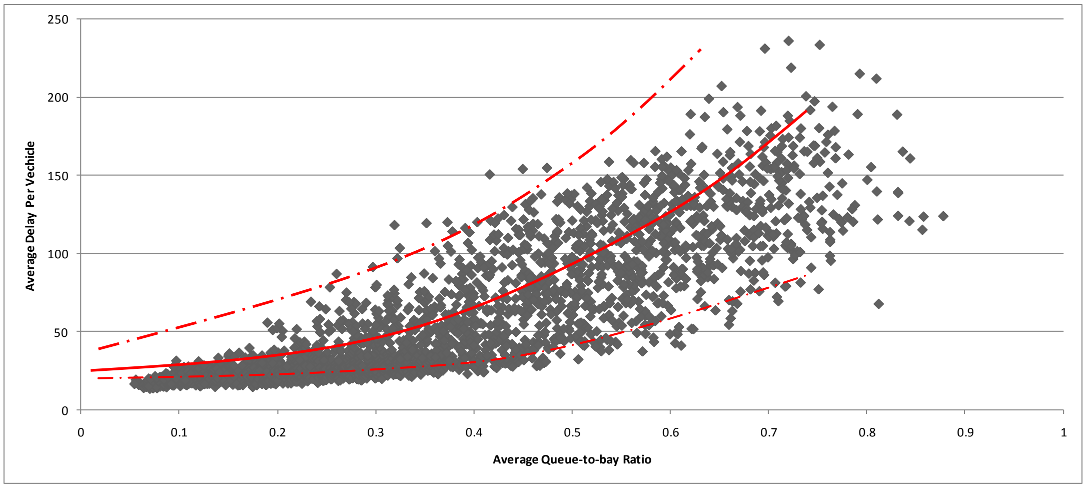

FIGURE 1(C) Scatter plot of average v.s. average QL Ratio

FIGURE 1(A)~(C) plotted the average delay per vehicle against several potential contribution factors. FIGURE 1(A) shows the relationship between the average delay and the total demand, revealing that both the mean value and the variance of delay increase linearly with the total intersection volume. FIGURE 1(B) presents the relationship between average delay and the average critical lane volume of CFI. The critical lane volume (CLV) is an indicator of the total conflicting flows within an intersection. Since a full CFI consists of five sub intersections, one can measure the congestion level of such a small signalized network with the arithmetic mean of CLV from each sub intersection. FIGURE 1(B) shows a clear exponential relation between the average delay and average CLV. The variance of the average delay also increases with CLV, where the distribution of delay points becomes widely spread at the high volume range.

FIGURE 1(C) illustrates the relationship between the average delay and queuing size within CFI. The QL ratio is defined as the ratio between the maximum queue length and the available bay (or link) length, i.e.,

$$\text{QL ratio } = \frac{\text{Maximum Queue Length}}{\text{Bay Length}} \tag{3}$$

If QL ratio of a bay is less than one, it indicates that the design can provide a sufficient storage capacity to accommodate all volumes approaching the target bay. In contrast, if it is greater than one, queue spillback may incur at that link due to insufficient bay capacity, and the service quality of the entire system may be deteriorated. The average QL ratio is defined as the arithmetic mean of all QL ratios within the CFI design. Similar to the critical lane volume which reflects the saturation level of an intersection, the average QL ratio measures the degree of queue formation with respect to all available bays. Both the mean value and variance of the average delay grow exponentially when the average QL ratio approaches one. The above three experimental results reveal the following critical relationships for our model development:

1) The average delay of CFI depends not only on the total volume, but also the geometric features of the intersection;
2) Comparing with the total volume, the CLV of each sub intersection is a reliable indicator to reflect the delay, especially under high congested conditions; and

3) The QL ratio has significant impacts on the CFI delay. When the average QL ratio of CFI increases, both the mean and variance of the average delay grows exponentially.

QUEUE LENGTH ESTIMATION

In view of the high correlation between QL ratios and average intersection delay, this section presents queue estimation model for each type of bays using a full CFI as an illustrative case. A full-CFI intersection is the most complex and comprehensive design in the CFI family. FIGURE 2 shows the classification of all possible queue types based on the geometric features of CFI. This study has calibrated the following four equations for those four types of queue at a full-CFI intersection, based on the data generated from extensive simulation experiments:

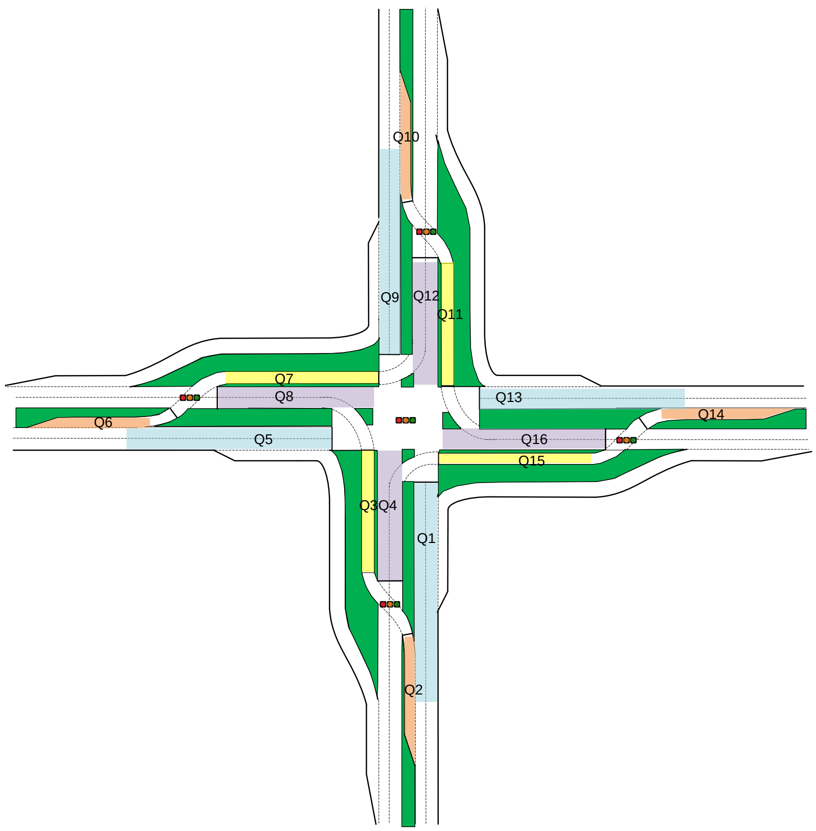

Type-1 Queue (Q_1, Q_5, Q_9, Q_{13}): Through queues at the major intersection;
Type-2 Queue (Q_2, Q_6, Q_{10}, Q_{14}): Left-turn queues at the crossover intersection;
Type-3 Queue (Q_3, Q_7, Q_{11}, Q_{15}): Left-turn queues at the major intersection;
Type-4 Queue (Q_4, Q_8, Q_{12}, Q_{16}): Through queues at the crossover intersection;

FIGURE 2 Spatial distribution of potential queue location at CFI

Base on the data from simulation experiments, the following queue models are developed with regression.

Type-1 Queue Model (Q_1, Q_5, Q_9, Q_{13})

The results of extensive simulations experiments indicate that the following factors may significantly impact the formation and dissipation of Type-1 queue: the approaching demand to the target approach, the green time ratio, and the intersection congested level measured with the critical lane volume (CLV). Hence, this study has employed these three factors to calibrate the following Type-1 queue model:

$$\text{Queue}=0.92\gamma\frac{D_t(1-G_t)s}{s-D_t}+5.14\left(\frac{D_t}{s-CV_m}\right)^2+1.72e^{\theta\rho_d} \tag{4}$$

t value: (64.9) (126.3) (16.7)

$R^2=0.862$, Sample size N: 2400

where,

D_t: Approaching through volume (vehicles per hour);

G_t: Estimated green time ratio for through movements at the major intersection;

s : The critical lane capacity (i.e., maximum critical lane volume);

CV_m: The critical lane volume at the major intersection;

ρ_d: QL ratio at the downstream link;

γ: Model parameter, γ=0.694; and

θ: Model parameter, θ=4.

Note that the above formulation indicates that the queue will grow continuously if the intersection critical lane volume has reached its capacity.

Type-2 Queue Model $(Q_2, Q_6, Q_{10}, Q_{14})$

Different from Type-1 queue, the formation of Type-2 queue is due mostly to the left-turn movement and is affected by the potential queue spillback at its downstream location. Thus, to explicitly account for the possible queue spillback, the research team has calibrated the following equation for Type-2 queue:

$$\text{Queue}=1.03\gamma\frac{D_l(1-G_l)s}{s-D_l}+6.28\left(\frac{D_l}{s-CV_n}\right)^2+1.13e^{\theta\rho_d} \tag{5}$$

t value: (234.8) (89.3) (8.6)

$R^2=0.877$, Sample size N: 2400

where,

D_l: Approaching left-turn volume (vehicles per hour);

G_l: Estimated green time ratio of left-turn movements at the crossover intersection;

s: The critical lane capacity (i.e., maximum critical lane volume);

CV_n: The critical lane volume at the crossover intersection;

ρ_d: QL ratio at the downstream link;

γ: Model parameter, γ=0.694; and

θ: Model parameter, θ=4.

Type-3 Queue $(Q_3, Q_7, Q_{11}, Q_{15})$

The formation of Type-3 queue varies with the green time at two neighboring signal intersections, as left-turn traffic flows, after crossing the opposing through traffic via the crossover intersection, need to pass the second signal at the primary junction where they can move concurrently with the through (or right-turn) traffic stream. Hence, we propose the following empirical equation for Type-3 queue:

$$\text{Queue}=0.729\gamma\left(1-\alpha\frac{D_l}{(s-D_l)}(1-G_u)\right)D_l+0.61e^{\theta\rho_d} \tag{6}$$

t value: (15.3) (29.7)

R^2=0.912, Sample size N: 2400

where,

D_l: Approaching left-turn volume (vehicles per hour);
G_u: Estimated green time ratio of left-turn movements at crossover intersections;
S: The critical lane capacity (i.e., maximum critical lane volume);
ρ_d: QL ratio at the downstream link;
γ: Model parameter, γ=0.694;
θ: Model parameter, θ=4; and
α: Model parameter, α=0.8;

Type-4 Queue $(Q_4, Q_8, Q_{12}, Q_{16})$

Similar to Type-1 queue, key factors such as the incoming demand to the target approach, the green time ratio, and the intersection congested level measured with the CLV can influence the formation of Type-4 queue. In addition, two approaching volumes should also be taken into account in the model development. By including all these factors, this study proposes the following Type-4 queue estimation model:

$$\text{Queue}=0.78\gamma\frac{(\beta D_t+D_l)(1-G_t)s}{s-(\beta D_t+D_l)}+5.62\left(\frac{\beta D_t+D_l}{s-CV_n}\right)^2 \tag{7}$$

t value: (82.7) (56.3)

R^2=0.817, Sample size N: 2400

where,

D_t: Incoming south (north) bound through volume (vehicles per hour);
D_l: Incoming west (east) bound left-turn volume (vehicles per hour);
CV_n: The critical lane volume at the crossover intersection;
G_t: Green time ratio for the through movement at the crossover intersection;
s: The critical lane capacity (i.e., maximum critical lane volume);
γ: Model parameter, γ=0.694; and
β: Model parameter, β=0.73.

Stability Tests of Queue Models

To further investigate the statistical property of the queue formulas derived from regression, two types of statistical tests have been performed: Shapiro-Wilk test of normality and Chow test of model stability. Shapiro-Wilk test is employed to confirm the estimation error of each queue model follows a normal distribution. As shown in TABLE 3, all queue models meet the normality test criterion which implies that the residuals of regression equations follow a normal distribution.

TABLE 3 Shapiro-Wilk Normality Test Results

Queue Model	Type 1	Type 2	Type 3	Type 4
W test statistic	0.9855	0.9767	0.9983	0.9972
P-Value	1.45e-17	1.72e-22	1.63e-3	1.38e-5

To evaluate the model's stability, Chow test is applied to verify that the coefficient of regression equations does not vary with the sample size. We divide the original dataset of 800 samples into two sub groups with n_1 and n_2 samples, and compute the following Chow test statistics:

$$F^* = \frac{\left[\sum e_p^2 - (\sum e_1^2 + \sum e_2^2)\right]/K}{(\sum e_1^2 + \sum e_2^2)/(n_1+n_2-2K)}$$

(8)

where, $\sum e_p^2, \sum e_1^2, \sum e_2^2$ is the sum of residual square of the regression model fitted with the original, group 1 and group 2 datasets; K is the number of parameters in regression;

The result of stability tests reflects that all estimated model parameters are statistically stable, implying that the estimated queue lengths with the proposed models are statistically reliable for use at the planning stage.

PLANNING MODEL FRAMEWORK

According to the above discussion, the occurrence of blockage at CFI may lead to a significant increasing of delay, and consequently a reduction of its operation benefits. With the queue estimation models, a planning framework is proposed to help engineers design CFI's link length, so as to prevent the potential queue spillback.

Demand Pattern and Signal Settings

Adopting the proposed queue models for estimation, two important components need to be discussed in detail: input demand and signal settings (i.e., green ratios). For the concern of traffic fluctuation, a successive design model should not rely on one exactly demand pattern. Therefore, a set of intervals are introduced to represent the traffic demand variations:

$$\mathbf{D} = \{\boldsymbol{\lambda}_i; \quad \forall i\} \tag{9}$$

where $\boldsymbol{\lambda}_i$ is a demand interval and $\boldsymbol{\lambda}_i = [\underline{\lambda}_i, \overline{\lambda}_i]$.

Due to the unique geometry features of CFI design, as one of the major operation benefits, a simple two phase signal strategy for CFI is presented in FIGURE 3.

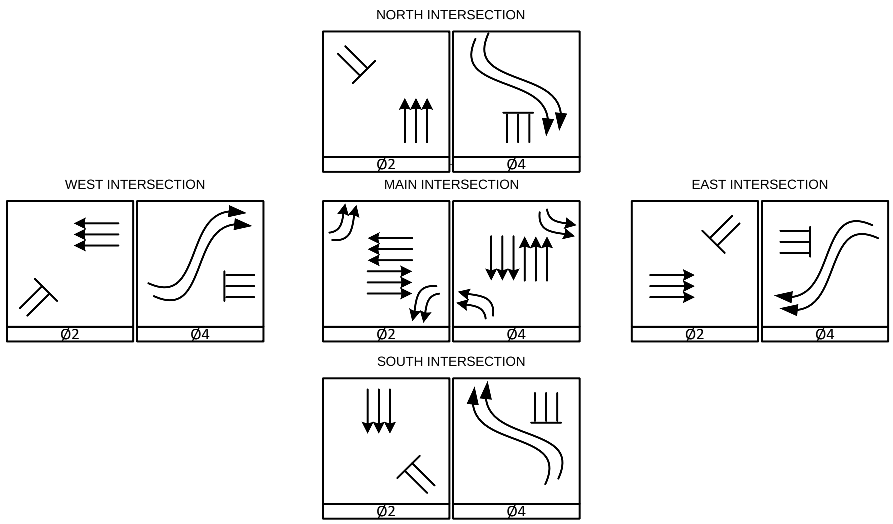

FIGURE 3 Signal phase diagram of a full CFI

At the planning stage, the preliminary signal settings are used for queue estimation only. Therefore, a simple and efficient way is adopted for signal design and a more in-depth signal optimization model would be introduced in future works. Given the demand pattern, the green ratio for movement *i* is computed by:

$$\mathbf{g}_i = \frac{\max\{\boldsymbol{\lambda}_i, \boldsymbol{\lambda}_j;\, j \in V_i\}}{\max\{\boldsymbol{\lambda}_i, \boldsymbol{\lambda}_j;\, j \in V\} + \max\{\boldsymbol{\lambda}_i, \boldsymbol{\lambda}_j;\, j \notin V\}} \quad \text{for each intersection j;} \tag{10}$$

where, $\boldsymbol{\lambda}_i$ is the demand of movement *i*; and V_i is the set of movements which obtain the right-of-way simultaneously with *i*.

Planning Process

As shown in FIGURE 2, 16 critical links are identified in a full CFI design. For a proper geometry design, the link length should be sufficient to store the potential traffic queues. With the proposed queue estimation models, the queue length could be estimated as follows:

$$\mathbf{Q}_i = f(\boldsymbol{\lambda}_i, \mathbf{g}_i) = [f(\underline{\lambda}_i, \overline{g}_i), f(\overline{\lambda}_i, \underline{g}_i)] \tag{11}$$

where $f(.)$ indicates the queue estimation model, and interval $\boldsymbol{Q}_i$ denotes the estimated queue length.

Note that in a real world application, the actual queue length may be shorter than the estimated result due to the coordinate of signal controllers. Therefore, to prevent of a conservative design, each link length of CFI is determined by:

$$L_i \geq \eta(\underline{Q}_i + \mu(\overline{Q}_i - \underline{Q}_i)) \tag{12}$$

where, $\mu, \eta \in (0,1)$.

Also note that the local construction environment can limit the design of link length. For instance, the distance to adjacent intersections will limit the length of CFI legs. Alternatively, another way is to increase the number of lanes for the particular link when the potential traffic queue exceeds its upper bound.

Overall, a planning framework is proposed for the geometry design of CFI and the process is represented by FIGURE 4.

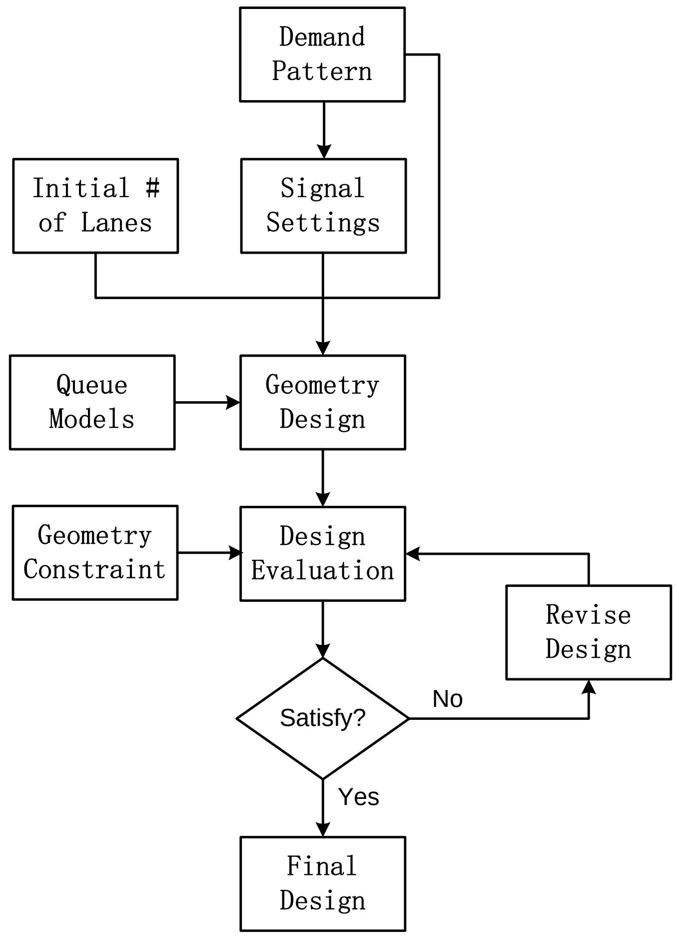

FIGURE 4 The flowchart of the planning framework

CASE STUDY

To evaluate the proposed planning framework, a real-world case is studied in this section. At the intersection of MD 4 and MD 235, Maryland SHA realizes the current conventional intersection cannot satisfy the increasing traffic demand during peak periods. Base on above discussions, a well designed CFI may help to release traffic congestion, considering its operational benefits. FIGURE 5 shows the current design and the layout of the proposed CFI design.

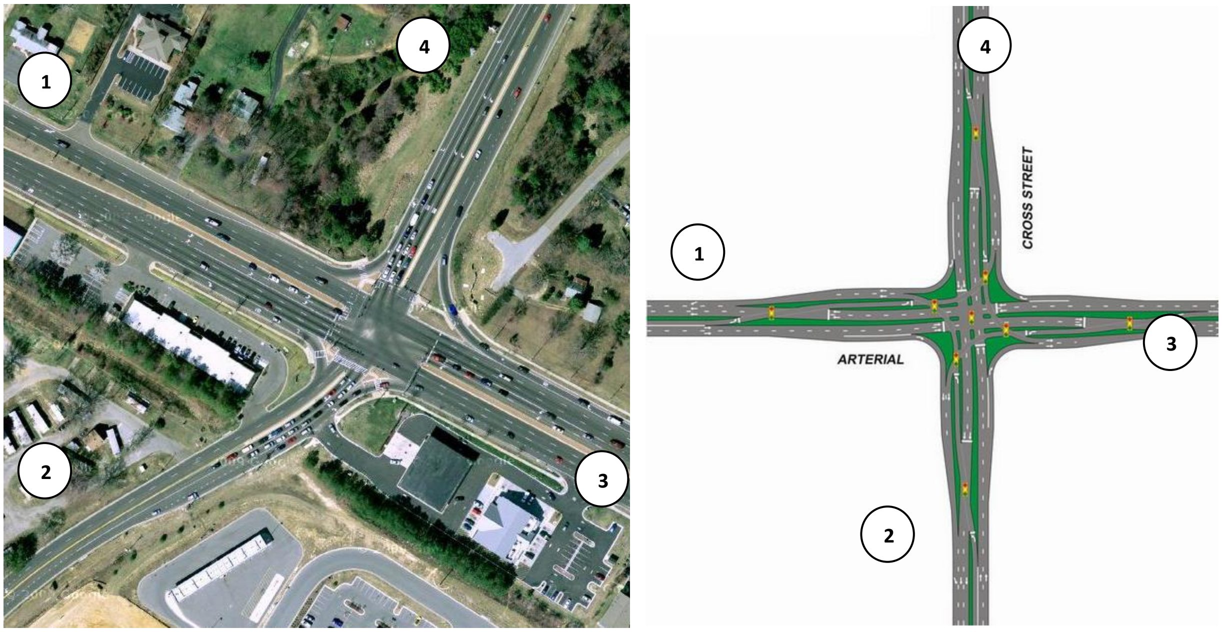

The bird view of the current intersection **The proposed continuous flow intersection**

FIGURE 5 The geometry design of intersection MD 4 @ MD 235

The proposed design is a full CFI which can contend with the heavy and unbalanced traffic volumes during the peak hours. The AM and PM peak hour traffic demands for this site are collected by the field survey, which can be further used to set the demand intervals, as shown in TABLE 4.

TABLE 4 AM and PM Peak Hour Demand and Demand Interval

Direction	Left-turn (veh/h)		Through (veh/h)		Right-turn (veh/h)	
	AM/PM	Interval	AM/PM	Interval	AM/PM	Interval
Eastbound	250/575	[250,575]	2475/1675	[1675,2475]	75/125	[75,125]
Northbound	100/125	[100,125]	250/425	[250,425]	350/200	[200,350]
Westbound	175/400	[175,400]	1150/2325	[1150,2325]	475/1375	[475,1375]
Southbound	1700/825	[825,1700]	325/400	[325,400]	450/375	[375,450]]

Some key parameters are set as follows:

- The maximum link length for the crossover space is 500 feet;
- The maximum link length for the left-turn bay is 550 feet;
- Leg 1: 2 lanes for left-turn link, 3 lanes for through link and 1 lane for right-turn link;
- Leg 2: 1 lanes for left-turn link, 2 lanes for through link and 1 lane for right-turn link;
- Leg 3: 2 lanes for left-turn link, 3 lanes for through link and 2 lane for right-turn link;
- Leg 4: 3 lanes for left-turn link, 2 lanes for through link and 1 lane for right-turn link;
- The constant parameter μ is assumed to be 0.6 and η is 0.8.

Follow the procedure of the planning framework, we firstly applied the proposed planning models to estimate the potential queue length, and the estimation results are used to determine the link length. Denote L1 as the left-turn bay (Q2, Q6, Q10, Q14 in FIGURE 2), L2 as the left-turn crossover link (Q3, Q7, Q11, Q15 in FIGURE 2), T1 as the through crossover link (Q4, Q8, Q12, Q16 in

FIGURE 2), and T2 as the through link (Q1, Q5, Q9, Q13 in FIGURE 2). The initial design settings are listed in TABLE 5:

TABLE 5: Initial Design of CFI

Location		**# of Lanes**	**Estimated Queue (ft)**	**Designed Link (ft)**	**Max Link Length (ft)**	**Satisfy**
Leg 1	L1	2	[76,252]	250	550	Yes
	T1	3	[84,260]	300	500	Yes
	L2	2	[52,112]	250	500	Yes
	T2	3	[351,707]	550	1050	Yes
Leg 2	L1	1	[109,133]	200	550	Yes
	T1	2	[134,217]	200	500	Yes
	L2	1	[112,231]	200	500	Yes
	T2	2	[129,197]	400	1050	Yes
Leg 3	L1	2	[73,99]	250	550	Yes
	T1	3	[69,152]	300	500	Yes
	L2	2	[64,140]	300	500	Yes
	T2	3	[121,585]	550	1050	Yes
Leg 4	L1	3	[120,347]	300	550	Yes
	T1	2	[400,620]	**550**	**500**	**No**
	L2	3	[60,212]	**550**	**500**	**No**
	T2	2	[35,51]	850	1050	Yes

*Note: the length of T2 is the sum of L1 length and L2 (or T1) length; and the length of T1 is equal to L2 Length.

As shown in TABLE 5, some designed link length cannot satisfy the maximum link length constraint, therefore, we increase the corresponding number of lanes at that location. The final design plan is represented in the TABLE 6:

TABLE 6: Final Design of CFI

Location		# of Lanes	Estimated Queue (ft)	Designed Link (ft)	Max Link Length (ft)	Feasible
Leg 1	L1	2	[76,252]	250	550	Yes
	T1	3	[84,260]	300	500	Yes
	L2	2	[52,112]	250	500	Yes
	T2	3	[351,707]	550	1050	Yes
Leg 2	L1	1	[109,133]	200	550	Yes
	T1	2	[134,217]	200	500	Yes
	L2	1	[112,231]	200	500	Yes
	T2	2	[129,197]	400	1050	Yes
Leg 3	L1	2	[73,99]	250	550	Yes
	T1	3	[69,152]	300	500	Yes
	L2	2	[64,140]	300	500	Yes
	T2	3	[121,585]	550	1050	Yes
Leg 4	L1	3	[120,347]	300	550	Yes
	T1	**3**	[201,370]	350	500	Yes
	L2	3	[60,212]	350	500	Yes
	T2	2	[35,51]	650	1050	Yes

With the revised geometry parameter, VISSIM is used as the unbiased platform to evaluate the designed CFI and current conventional intersection. TABLE 7 summarizes the performance comparison between these two designs. Average number of vehicle stops and average network delay are the selected MOEs.

TABLE 7 Performance Comparisons between Different Scenarios

Time	Design	Ave. # of Stops	Improvement	Ave. Delay	Improvement
AM peak hours	Current design	3.12	/	77.2	/
	Proposed CFI design	2.39	-23.4%	48.6	-37.04%
PM peak hours	Current design	2.98	/	63.4	/
	Proposed CFI design	2.02	-32.2%	41.3	-34.5%

From TABLE 7, one can observe a significant reduction of both average number of vehicle stops and average delay within the CFI design. There are two plausible reasons for having such improvements. First, the CFI design eliminates the left-turn flows from the through volume, which consequently reduces the number of signal phase and improves the level of service at the center intersection. Secondly, the CFI has a larger geometry layout to prevent the occurrence of queue spillbacks. Also, to a certain extent, the MOEs improvement of CFI can reveal the effectiveness of the design framework.

To further evaluate the design plan shown in TABLE 6, 70 demand patterns within the input demand intervals are randomly generated in VISSIM. Since a proper design shall offer sufficient link length to store the potential traffic queue, the defined QL ratio is selected as the direct indicator of blockage. FIGURE 6 presents the average and maximum QL ratio over 70 scenarios at each critical location.

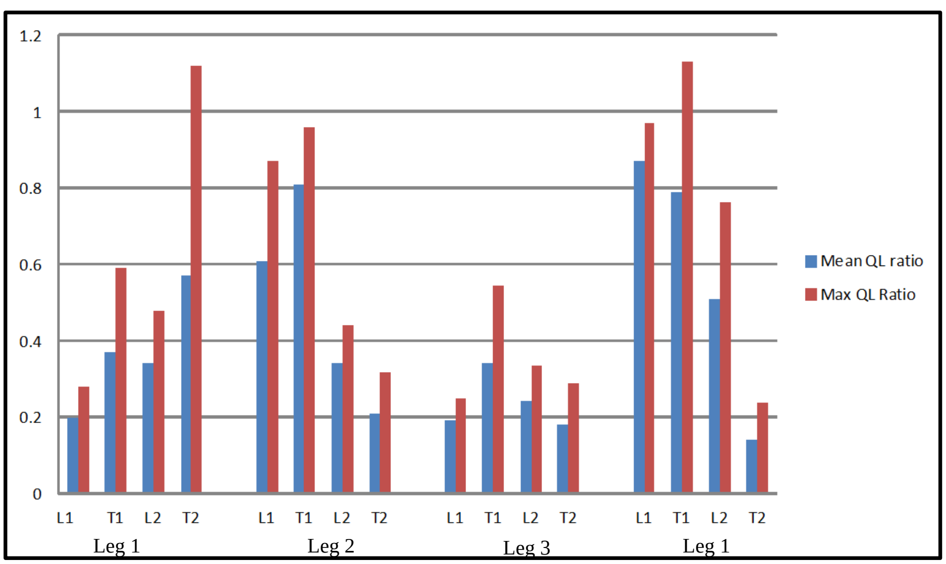

FIGURE 6 The evaluated QL ratios (Mean and Max)

Obviously, one can observe that the designed links are sufficient to storage the traffic queue for most cases (the mean QL ratios are smaller than 1.0), revealing the effectiveness of the proposed planning framework. Also note that the max QL ratio exceeds 1.0 at Leg1-T2 and Leg 4-T1, which indicates the occurrence of blockage. However, to prevent of a conservative design and for the consideration of land use and construction cost, there is no need to extend the link length at Leg1-T2 and Leg 4-T1. Since the QL ratio is small at other links, an alternative way to prevent the potential blockage is to revise the signal settings and increase the green time of the congested movements.

CONCLUSION

This paper proposed a planning framework for CFI's geometry designs. Due to the interdependent nature of traffic queues among a CFI's five closely-spaced intersections, the proposed framework specifically include a QL ratio as a key variable, offering an effective and convenient way for users to identify any potential queue spillback location. Based on the experimental data, a performance analysis for CFI's delay is performed, revealing the inter-correlation between delay and QL ratio at each critical location. To generate a proper design plan and to prevent the potential queue blockage, a set of queue estimation models are developed using regression. Based on the validated queue models, a clear design framework is enable users to compute the link length at both through and left-turn locations in CFI.

Recognizing the limit of available real-world data, this study has employed microscopic simulation results for model development, and concluded that both delays and queues yielded from our proposed models are sufficient for preliminary design such as assessing if traffic queue may spill back at a target bay or not. Our on-going research is to further investigate the complex interrelations between the queue formation and dissipation among a CFI's five intersections under various signal control plans. The results of delay and queue analyses at the operational level will serve as the basis for our development of a special network signal model for CFI.

ACKNOWLEDGEMENT

Here authors are appreciated for data support from the Maryland State Highway Administration and express deepest appreciations to Mr. Yang Lu who made contributions in the data processing.

REFERENCES

1. Goldblatt, R.F., Mier, F. and Friedman, J., 1994. Continuous Flow Intersection, Institute of Transportation Engineers Journal, 64 (7), pp 34-42.
2. Hummer, J.E., 1998. Unconventional Left-Turn Alternative for Urban and Suburban Arterials: Part Two. ITE Journal on the Web, pp. 101-106.
3. Reid,J. D., Hummer,J. E., 1999. Analyzing System Travel Time in Arterial Corridors with Unconventional Designs Using Microscopic Simulation. Transportation Research Record, 1678, pp.208-215.
4. Hummer, J.E., 1998. Unconventional Left-Turn Alternative for Urban and Suburban Arterials: Part One. ITE Journal, 68 (9), pp. 26-29.
5. Reid,J. D., Hummer,J. E., 2001. Travel Time Comparisons between Seven Unconventional Arterial Intersection Designs. Transportation Research Record, 1751, pp.55-56.
6. Jagannathan, R., Bared, J. G., 2004. Design and Operational Performance of Crossover Displaced Left-Turn Intersections. Transportation Research Record, 1981, pp.86-96.
7. Cheong S., Rahwanji S., Chang G.L., 2008. Comparison of Three Unconventional Arterial Intersection Designs: Continuous Flow Intersection, Parallel Flow Intersection, and Upstream Signalized Crossover. 11th International IEEE Conference.
8. Kim, M., Lai, X., Chang G.L., Rahwanji, S., 2007. Unconventional Arterial Designs Initiatives. Presented at IEEE Conference on Intelligent Transportation Systems, Seattle.

9. Mohamed EI Esawey and Tarek Sayed, 2007. Comparison of Two Unconventional Intersection Schemes. Transportation Research Record, No 2023, pp 10-19
10. Pitaksringkarn, J. P., 2005. Measures of Effectiveness for Continuous Flow Intersection: A Maryland Intersection Case Study. ITE 2005 Annual Meeting and Exhibit Compendium of Technical Papers.
11. FHWA, US Department of Transportation, 2010. Alternative Intersections/Interchanges: Information Report (AIIR).
12. Esawey, M.E., Sayed, T., 2007. Comparison of Two Unconventional Intersection Schemes. Transportation Research Record, 2023, pp. 10-19.
13. Hildebrand, T. E., 2007. Unconventional Intersection Designs for Improving Through Traffic Along The Arterial Road. A Thesis Submitted to the Department of Civil and Environmental Engineering, the Florida State University.
14. Inman, V. W., 2009. Evaluation of Signs and Markings for Partial Continuous Flow Intersection. Transportation Research Record, 2138, pp. 66-74.